Steepest entropy ascent quantum thermodynamic model of electron and phonon transport

Guanchen Li,[1,*] Michael R. von Spakovsky,[1,2] and Celine Hin[1,3]

[1]*Department of Mechanical Engineering, Virginia Tech, Blacksburg, Virginia 24061, USA*
[2]*Center for Energy Systems Research, Department of Mechanical Engineering, Virginia Tech, Blacksburg, Virginia 24061, USA*
[3]*Department of Materials Science and Engineering, Virginia Tech, Blacksburg, Virginia 24061, USA*

An advanced nonequilibrium thermodynamic model for electron and phonon transport is formulated based on the steepest-entropy-ascent quantum thermodynamics framework. This framework, based on the principle of steepest entropy ascent (or the equivalent maximum entropy production principle), inherently satisfies the laws of thermodynamics and mechanics and is applicable at all temporal and spatial scales even in the far-from-equilibrium realm. Specifically, the model is proven to recover the Boltzmann transport equations in the near-equilibrium limit and the two-temperature model of electron-phonon coupling when no dispersion is assumed. The heat and mass transport at a temperature discontinuity across a homogeneous interface where the dispersion and coupling of electron and phonon transport are both considered are then modeled. Local nonequilibrium system evolution and nonquasiequilibrium interactions are predicted and the results discussed.

I. INTRODUCTION

Nonequilibrium phenomena exist at all temporal and spatial scales and play an important role in deciding device performance. Many different types of microscopic and mesoscopic models describing nonequilibrium phenomena have been developed [1–10], but they are all limited with respect to their general applicability to the nonequilibrium realm. Studying these phenomena at larger scales with macroscopic continuum models [11–16] is theoretically even more limited. The general procedure for including nonequilibrium effects in continuum models consists of two general steps, both of which suffer from an incomplete or inadequate description of the nonequilibrium system. The first is to approximate the nonequilibrium state of the system using a fine mesh of local systems each of which is assumed to be in a state of local equilibrium. However, such a mesh is limited in its ability to describe each actual local state, which is that of nonequilibrium. The second step is to address the nonequilibrium effects of the system dynamics, i.e., transports, via the inclusion of a set of phenomenological coefficients (e.g., diffusivity, thermal and electrical conductivities, viscosity, etc.). However, these coefficients are often based on uncoupled behavior and if not are still limited to the linear regime and are, thus, not generally applicable and must be determined independently via measurements or a microscopic or mesoscopic model. The latter can be used to provide a set of linear (as opposed to nonlinear) coefficients based on the energy and mass flows resulting from a set of master equations (i.e., microscopic or mesoscopic equations of motion). However, the actual transport of interest may be nonlinear and, thus, the coefficients developed via the microscopic or mesoscopic model inadequate. Furthermore, determining these coefficients is only possible between two local equilibrium

systems, since the intensive properties used to determine them are only defined at equilibrium. A specific illustration of this is found in nonequilibrium molecular dynamics (NEMDs) where heat transfer at the interface between two materials is modeled [17] by attaching the two sides of the interface to two different thermal reservoirs. The thermal interface conductance is then determined as a function of the temperatures of the reservoirs. Thus, without the local equilibrium assumption both at the microscopic or mesoscopic level in determining the phenomenological coefficients and at the macroscopic level in solving the equations for mass and energy transport, the continuum model fails and is unable to predict how a nonquasiequilibrium process produces a nonlocal equilibrium state.

The incompleteness of the nonequilibrium state description also exists at the mesoscopic level when the kinetic theory model is used in the far-from-equilibrium realm. The reason is that outside of the near-equilibrium realm, using only the conservation laws is insufficient for providing a closed system of transport equations for a system's properties, which are evaluated via moments of a probability distribution function [10]. The closure problem results from the fact that if system state evolution, which would theoretically be determined via complex microscopic interactions represented by collision integrals, were instead evaluated without these, a closed description would require additional information, in particular that for entropy generation. An attempt to provide closure comes from extended thermodynamics [14], which uses the principle of maximum entropy production (MEP). In doing so, the distribution function is used to calculate higher-order moments, and the entropy production term is assumed to be that which maximizes the entropy under the given constraints [18,19]. However, such an approach appears to be more of a practical one than a fundamental one, since it neither provides a general equation of motion for the nonequilibrium realm nor attempts to investigate the entropy generation process in the evolution of an arbitrary nonequilibrium state.

---

*guanchen@vt.edu

Of course, complex microscopic interactions can be used directly to predict the evolution of individual energy levels via a collision or scattering process based on Newton's law or quantum mechanics as is done with the Boltzmann transport equations (e.g., [20]) or with nonequilibrium Green's functions (e.g., [3]), respectively. The evolution of system thermodynamic properties can then be developed within certain limits from the microscopic process, although it must be emphasized that in the case of Green's functions the laws of thermodynamics are not inherently satisfied and satisfying them is very sensitive to the level of approximation used, while the applicability of BTE to regions other than the near-equilibrium is limited by its local-equilibrium requirement.

To address all of the above deficiencies, an advanced nonequilibrium thermodyanmics-ensemble based framework called steepest-entropy-ascent quantum thermodynamics (SEAQT) provides a general thermodynamically rigorous equation of motion for nonequilibrium system state evolution. It bases the relaxation of system state on the conservation laws of thermodynamics and on the principle of steepest entropy ascent (SEA) [21–39]. With the development of the concept of hypoequilibrium state and the density-of-states method [27–30], SEAQT can be applied from a practical standpoint at all temporal and spatial scales. Unlike conventional methods such as the ones described above, the SEAQT framework provides an equation of motion that can be used to investigate the evolution of local nonequilibrium states from an entropy generation standpoint. The concept of hypoequilibrium further simplifies this nonequilibrium description via the use of nonequilibrium intensive properties (e.g., temperature and pressure) and extends the thermodynamic equilibrium description (e.g., the Onsager relations, the Gibbs relation, etc.) into the nonequilibrium realm, even that far from equilibrium. Thus, using SEAQT, nonequilibrium state evolution can be described completely for any macroscopic or mesoscopic system via a set of extensive and intensive thermodynamic properties using a closed system of equations of motion for these properties.

In this paper, the SEAQT framework is applied to the study of the mass and energy transport of electrons and phonons at a temperature discontinuity across a homogeneous interface (i.e., an interface with the same material on either side but with each side at a different temperature). Unlike conventional methods [40], which in general rely on either kinetic theory at the mesoscopic scale [20] or classical mechanics (NEMD [17]) and quantum mechanics at the microscopic scale (e.g., atomistic Green's functions [41] and nonequilibrium Green's functions [3]), the SEAQT description provides details at multiple levels, i.e., in this case both at the macroscopic and mesoscopic levels, and emphasizes the general thermodynamic features of state evolution without requiring explicit details of the mechanical interactions (e.g., particle collisions). This is the case since the history of the intermediate states of the relaxation process does not depend on the overall time scale of the evolution (i.e., on the actual dynamics and not even on the relaxation time selected when a single relaxation time is involved). In other words, the nonequilibrium trajectory predicted is a static path in thermodynamic state space, which does not depend on how fast the evolution occurs. Furthermore, by accounting for the temperature discontinuity across a homogeneous interface only, the influence of material properties (e.g.,

lattice mismatch [42], band-structure alignment [43], intrinsic defects [44,45], and stress [46]) has purposely been removed in order to illustrate how the SEAQT framework can be used to predict the universal nonequilibrium thermodynamic features of the interfacial mass and heat transfer with electron-phonon coupling. Nonetheless, this framework can be utilized to study the heterointerface structure and properties with input data such as the system's eigenstructure calculated with density functional theory (DFT) or NEMD. This, however, is beyond the scope of the present paper.

The paper is organized as follows. In Sec. II, the SEAQT framework is briefly described and the equation of motion derived from the SEA principle. Section III provides a brief explanation of the hypoequilibrium concept. Using this concept, the SEAQT equation of motion can be simplified significantly and solved very practically. Section IV then follows with a thermodynamically rigorous derivation of the SEAQT transport equations for electron and phonon transport applicable even in the far-from-equilibrium realm. Moreover, it is shown that these transport equations can recover the Boltzmann transport equation in the near-equilibrium realm. Finally, Sec. V applies the SEAQT framework to the study of heat and mass transport at a temperature discontinuity across a homogeneous interface. The nonquasiequilibrium process at the interface as well as the relaxation of the local nonequilibrium systems are studied.

II. STEEPEST-ENTROPY-ASCENT FRAMEWORK

The equation of motion for moving through thermodynamic state space is derived using the SEA principle [25,47]. In the system, there are m single-particle energy eigenlevels $\{\epsilon^k, \ k = a, \dots, m\}$ that can be occupied by particles. A system eigenstate is denoted using the occupation number representation $|n^a n^b \dots n^m\rangle$ where n^k is the occupation number at the kth single-particle eigenlevel ϵ^k. n^k is valued $0,1$ for fermions and $0,1,\dots,\infty$ for bosons. A system thermodynamic state is selected from the Hilbert space spanned by the system eigenstates and can be represented equivalently by a w-dimensional vector $\{p_{n^k}^k\}$. The vector element $p_{n^k}^k$ represents the probability that n^k particles are observed at the kth single-particle eigenlevel where $k = a, \dots, m$. The explicit form of the w-dimensional vector is

$$\text{fermion}: \left\{ p_{n^a=0}^a, p_{n^a=1}^a, p_{n^b=0}^b, p_{n^b=1}^b, \dots, p_{n^m=1}^m \right\}, \quad (1)$$

$$\text{bosons}: \left\{ p_{n^a=0}^a, \dots, p_{n^a=\infty}^a, p_{n^b=0}^b, \dots, \right.$$
$$\left. p_{n^b=\infty}^b, \dots, p_{n^m=0}^m, \dots, p_{n^m=\infty}^m \right\}, \quad (2)$$

where the total dimension of the vector is $w = 2m$ for fermions and $w = \infty$ for bosons.

To facilitate the imposition of the constraints discussed later, the system thermodynamic state can alternatively be denoted by using the square root of the vector $\{p_{n^k}^k\}$ such that

$$\gamma = \text{vect}(\gamma_{n^k}^k) \equiv \text{vect}(\sqrt{p_{n^k}^k}), \quad k = a, \dots, m;$$

$$n^k = 0,1 \text{ for fermion and } 0,1,\dots,\infty \text{ for boson}. \quad (3)$$

The thermodynamic state space of the system, i.e., the γ space, can then be defined as a manifold whose elements are all of the w vectors of the real finite numbers $X = \text{vect}(x_l)$ and

$Y = \text{vect}(y_l)$ equipped with an inner product $(\cdot|\cdot)$ given by

$$(X|Y) \equiv \sum_{l=1}^{w} x_l y_l. \qquad (4)$$

For a specific thermodynamic state represented by γ, the system properties can be defined by the functionals $\tilde{A}(\gamma)$, $\tilde{B}(\gamma), \ldots$ of γ [or the vector $|\gamma\rangle$]. The functional derivatives with respect to γ are $\delta\tilde{A}(\gamma)/\delta\gamma$. The time evolution of the thermodynamic state $\gamma(t)$ follows the equation of motion in w-vector form given by

$$|d\gamma/dt\rangle = |\Pi_\gamma\rangle. \qquad (5)$$

The formalism of $|\Pi_\gamma\rangle$ is derived from the SEA principle subject to a set of conservation laws $\{\tilde{C}(\gamma)\}$ to which the system yields. These include conservation of energy $\tilde{H}(\gamma) = \sum_k \sum_{n_k} n^k \epsilon_k p_{n^k}^k$ and of particle number $\tilde{N}(\gamma)$ as well as m probability normalization conditions $\tilde{I}_k(\gamma)$. Using Eq. (4), the time evolution of these conserved system properties $\{\tilde{C}(\gamma)\} = \{\tilde{H}, \tilde{N}, \tilde{I}_a, \ldots, \tilde{I}_m\}$ and the system entropy $\tilde{S}(\gamma)$ obey the following equations of motion:

$$\Pi_{C_i} \equiv dC_i/dt = (\Psi_i|\Pi_\gamma) = 0, \quad \text{with } |\Psi_i\rangle \equiv |\delta\tilde{C}_i(\gamma)/\delta\gamma\rangle, \qquad (6)$$

$$\Pi_S \equiv dS/dt = (\Phi|\Pi_\gamma) \geqslant 0, \quad \text{with } |\Phi\rangle \equiv |\delta\tilde{S}(\gamma)/\delta\gamma\rangle \qquad (7)$$

The time evolution of the system $|\Pi_\gamma\rangle$ corresponds to a trajectory in thermodynamic state space, which obeys the SEA variational principle. The corresponding variational problem consists of finding the instantaneous "direction" of $|\Pi_\gamma\rangle$, which maximizes the entropy production rate Π_S subject to the constraints $\Pi_{C_i} = 0$. To do so, the state space must be equipped with a metric field with which to compute the distance traveled during the evolution and the norm of Π_γ. The differential of the distance traveled along the path in state space is then expressed as

$$dl = \sqrt{(\Pi_\gamma|\hat{G}(\gamma)|\Pi_\gamma)}\, dt. \qquad (8)$$

where $\hat{G}(\gamma)$ is a real, symmetric, positive-definite operator on the manifold which defines the thermodynamic state space [25]. When $\hat{G}(\gamma)$ is the identity operator, the distance corresponds to the simplest measure, which is the Fisher-Rao metric. The SEA variational problem is now solved by maximizing the entropy production rate Π_S subject to the constraints $\Pi_{C_i} = 0$. The additional constraint $(dl/dt)^2$ is set equal to some small positive constant so that the norm of Π_γ is kept constant, as needed. The maximization occurs only with respect to its direction. The solution is found using the method of Lagrange multipliers where the Lagrangian is written as

$$\Upsilon = \Pi_S - \sum_i \beta_i \Pi_{C_i} - \frac{\tau}{2}(\Pi_\gamma|\hat{G}(\gamma)|\Pi_\gamma) \qquad (9)$$

and β_i and $\tau/2$ are the Lagrange multipliers. Taking the variational derivative of Υ with respect to $|\Pi_\gamma\rangle$ and setting

it equal to zero results in

$$\frac{\delta\Upsilon}{\delta\Pi_\gamma} = |\Phi\rangle - \sum_i \beta_i|\Psi_i\rangle - \tau\hat{G}|\Pi_\gamma\rangle = 0. \qquad (10)$$

Thus, the SEA equation of motion takes the form

$$|\Pi_\gamma\rangle = \hat{L}\left(|\Phi\rangle - \sum_i \beta_i|\Psi_i\rangle\right), \qquad (11)$$

where $\hat{L} \equiv \hat{G}^{-1}/\tau$ is assumed for purposes of this paper to be diagonal. As is shown below, the diagonal terms of $\hat{L}$ $\{\tau_{n^k}^k, k = 1, \ldots, m; n^k = 0,1$ for fermion, and $0,1,0,\ldots,\infty$ for bosons$\}$ are related to the relaxation times of system single-particle eigenlevels so that

$$\hat{L} = \text{diag}\left\{\frac{1}{\tau_{n^k}^k}\right\}. \qquad (12)$$

The values of the Lagrange multipliers, the β_i, are calculated by inserting Eq. (11) into the conservation laws expressed by Eq. (6), resulting in

$$\sum_{j=1}^{m+2} (\Psi_i|\hat{L}|\Psi_j)\beta_j = (\Psi_i|\hat{L}|\Phi). \qquad (13)$$

These β_j can be used to define the measurements of nonequilibrium system intensive properties (e.g., temperature, pressure, and chemical potential) [30].

Substituting the functional derivatives of the system properties given by Eqs. (A1)–(A4) in Appendix A into Eq. (11), the equations of motion for the γ^k and the $p_{n^k}^k$ of the probability distribution among the single-particle eigenlevels ϵ^k can be written as

$$\frac{d\gamma_{n^k}^k}{dt} = \frac{1}{\tau_{n^k}^k}\left(-\gamma_{n^k}^k \ln p_{n^k}^k - n^k\epsilon^k\gamma_{n^k}^k\beta_E - n^k\gamma_{n^k}^k\beta_N - \gamma_{n^k}^k\beta_I^k\right), \qquad (14)$$

$$\frac{dp_{n^k}^k}{dt} = \frac{1}{\tau_{n^k}^k}\left(-p_{n^k}^k \ln p_{n^k}^k - n^k\epsilon^k p_{n^k}^k\beta_E - n^k p_{n^k}^k\beta_N - p_{n^k}^k\beta_I^k\right), \qquad (15)$$

where k stands for the single-particle eigenlevel index and n^k for the occupation number at this level. β_E, β_N, and β_I^k are, respectively, the Lagrange multipliers corresponding to the generators of the motion $\hat{H}$, $\hat{N}$, and $\hat{I}_k$.

III. HYPOEQUILIBRIUM STATE

The hypoequilibrium concept developed in [27,28,30] can simplify the expression for the equation of motion and facilitates the physical interpretation [47] of the evolution in state. It is assumed without loss of any significant generality (see [27]) that the particles occupying the same single-particle eigenlevel ϵ are initially in mutual equilibrium with respect to the chemical potential μ^ϵ and temperature T^ϵ so that the initial probability distribution $p_{n^\epsilon}^\epsilon$ among the different occupation states is Maxwellian, i.e.,

$$p_{n^\epsilon}^\epsilon = \frac{e^{-\beta_N^\epsilon n^\epsilon - \beta_E^\epsilon n^\epsilon \epsilon}}{\Xi^\epsilon} = e^{-\beta_I^\epsilon - \beta_N^\epsilon n^\epsilon - \beta_E^\epsilon n^\epsilon \epsilon}, \qquad (16)$$

where $\beta_E^\epsilon \equiv 1/k_B T^\epsilon$ is defined by the temperature T^ϵ, $\beta_N^\epsilon \equiv \mu^\epsilon/k_B T^\epsilon$ by the chemical potential μ^ϵ, and $\beta_I^\epsilon \equiv \ln \Xi^\epsilon$ by the single-particle level partition function given by

$$\Xi^\epsilon\left(\beta_E^\epsilon, \beta_N^\epsilon\right) = \sum_{n^\epsilon}^{\infty} e^{-\beta_N^\epsilon n^\epsilon} e^{-\beta_E^\epsilon n^\epsilon \epsilon}. \qquad (17)$$

Such an initial state is called a hypoequilibrium state.

In addition, it is assumed that the different occupation states of the same single-particle eigenlevel have the same relaxation time, namely,

$$\tau_{n^\epsilon}^\epsilon = \tau^\epsilon \quad \text{for all } n^\epsilon \text{ in the same } \epsilon, \qquad (18)$$

which means that each relaxation time is a property of a given single-particle eigenlevel.

Under these two conditions, it is proven in [27,28,30,47] that the system remains in a hypoequilibrium state throughout the entire time evolution given by Eq. (15). As a consequence, the time evolution of the system can be determined via the motion of the state of a single-particle eigenlevel [47] defined by

$$y^\epsilon = \beta_N^\epsilon + \beta_E^\epsilon \epsilon. \qquad (19)$$

Substituting Eq. (16) into (15), the equation of motion for y^ϵ becomes

$$\frac{dy^\epsilon}{dt} = -\frac{1}{\tau^\epsilon}(y^\epsilon - \beta_E \epsilon - \beta_N). \qquad (20)$$

Multiplying Eq. (15) successively by the system extensive properties of particle number, energy, and entropy and integrating over n^ϵ, the contributions to these properties from a single-particle eigenlevel ϵ provide the following evolutions:

$$\frac{d\langle N \rangle_\epsilon}{dt} = \frac{1}{\tau^\epsilon} A_{NN}^\epsilon(y^\epsilon - \beta_E \epsilon - \beta_N). \qquad (21)$$

$$\frac{d\langle e \rangle_\epsilon}{dt} = \epsilon \frac{d\langle N \rangle_\epsilon}{dt}, \qquad (22)$$

$$\frac{d\langle s \rangle_\epsilon}{dt} = y^\epsilon \frac{d\langle N \rangle_\epsilon}{dt}, \qquad (23)$$

where $\langle N \rangle_\epsilon$, $\langle e \rangle_\epsilon$, and $\langle s \rangle_\epsilon$ are the expectation values of the particle number, energy, and entropy of the single-particle eigenlevel. A_{NN}^ϵ is the particle number fluctuation of the single-particle eigenlevel defined as

$$A_{NN}^\epsilon \equiv \langle N^2 \rangle^\epsilon - (\langle N \rangle^\epsilon)^2 = \frac{\partial^2}{\partial^2 \beta_N^\epsilon} \ln \Xi^\epsilon = -\frac{\partial \langle N \rangle^\epsilon}{\partial \beta_N^\epsilon}$$

$$= \frac{1}{e^y \pm 1} \mp \frac{1}{(e^y \pm 1)^2}, \qquad (24)$$

where fermions take the plus sign and bosons the negative.

IV. TRANSPORT EQUATIONS

A. Electron transport equation

In this section, Eq. (15) is applied to the study of the electron transport between two systems. The set of single-particle eigenlevels studied, $\{\epsilon^{A,k}, \epsilon^{B,l}\}$, is composed of the eigenlevels at location A $\{\epsilon^{A,k}\}$ and those at location B $\{\epsilon^{B,l}\}$. Integrating Eq. (21) over the energy eigenlevels of location A yields the

particle number evolution at this location given by

$$\frac{d\langle N \rangle^A}{dt} = \int \frac{V}{\tau^{A,\epsilon}} A_{NN}^{A,\epsilon}\left(\beta_E^{A,\epsilon}\epsilon + \beta_N^{A,\epsilon} - \beta_E\epsilon - \beta_N\right)D^A(\epsilon)d\epsilon, \qquad (25)$$

where $D^A(\epsilon)$ is the density of states per unit volume at location A determined as outlined in [27] and V is the volume.

In the near-equilibrium realm, it is assumed that systems A and B are both approximately in stable equilibrium, i.e.,

$$\beta_E^{A,\epsilon} = \beta_E^A, \qquad (26)$$

$$\beta_N^{A,\epsilon} = \beta_N^A \qquad (27)$$

(and similarly for B) so that for A

$$\frac{d\langle N \rangle^A}{dt} = \int \frac{V}{\tau^{A,\epsilon}}\left(\beta_E^A \epsilon + \beta_N^A - \beta_E\epsilon - \beta_N\right)A_{NN}^{A,\epsilon}D^A(\epsilon)d\epsilon$$

$$= \left(\beta_N^A - \beta_N\right)\int \frac{V}{\tau^{A,\epsilon}} A_{NN}^{A,\epsilon}D^A(\epsilon)d\epsilon$$

$$+ \left(\beta_E^A - \beta_E\right)\int \frac{V\epsilon}{\tau^{A,\epsilon}} A_{NN}^{A,\epsilon}D^A(\epsilon)d\epsilon. \qquad (28)$$

Moreover, the near-equilibrium assumption permits retention of the zeroth-order approximation for the terms inside the integrals so that only the first-order approximation of $d\langle N \rangle^A/dt$ is retained. In particular, it is assumed that systems A and B have the same energy eigenstructure so that the relaxation times and density of states of A and B are the same, i.e.,

$$\tau^{A,\epsilon} = \tau^{B,\epsilon} = \tau^\epsilon, \quad D^A(\epsilon) = D^B(\epsilon) = D(\epsilon). \qquad (29)$$

It is also assumed that the fluctuations of systems A and B are approximately equal to their mutual equilibrium value at (β_N, β_E), namely, that

$$A_{NN}^{A,\epsilon} = A_{NN}^{B,\epsilon} = A_{NN}^\epsilon(\beta_N, \beta_E). \qquad (30)$$

The particle flow from B to A is then found by subtracting from Eq. (28) the corresponding one for system B so that

$$\frac{d\langle N \rangle^A}{dt} - \frac{d\langle N \rangle^B}{dt} = 2\frac{d\langle N \rangle^A}{dt}$$

$$= \left(\beta_N^A - \beta_N^B\right)\int \frac{V}{\tau^\epsilon} A_{NN}^\epsilon D(\epsilon)d\epsilon$$

$$+ \left(\beta_E^A - \beta_E^B\right)\int \frac{V\epsilon}{\tau^\epsilon} A_{NN}^\epsilon D(\epsilon)d\epsilon, \qquad (31)$$

where the term to the right of the first equal sign is the result of particle conservation, i.e., $d\langle N \rangle^A/dt + d\langle N \rangle^B/dt = 0$. Defining

$$\delta[\beta_E(\epsilon + \mu)] = \left(\beta_N^A + \epsilon\beta_E^A\right) - \left(\beta_N^B + \epsilon\beta_E^B\right), \qquad (32)$$

where $\mu \equiv \beta_N/\beta_E$ and using Eq. (31), the total particle flow to A can be written as

$$AJ_N \equiv 2\frac{d\langle N \rangle^A}{dt} = \int \delta[\beta_E(\epsilon + \mu)]\frac{V}{\tau^\epsilon} A_{NN}^\epsilon D(\epsilon)d\epsilon. \qquad (33)$$

Here A is the cross-sectional area of the interface separating systems A and B. J_N is the particle flux across the interface between system A and B. If system A is part of a series of local systems, the flow along a given direction for A is given by the

contributions from two interfaces, which results in the factor 2 after the first equal sign in Eq. (34). By using the following variational relation for every energy level ϵ:

$$\delta[\beta_E(\epsilon + \mu)] = \left((\epsilon + \mu)\frac{d\beta_E}{dx} + \beta_E\frac{d\mu}{dx}\right)\delta x, \qquad (34)$$

where δx is the distance between the locations A and B, Eq. (33) can be rewritten as

$$AJ_N = \delta x \int \frac{V}{\tau^\epsilon}\left((\epsilon + \mu)\frac{d\beta_E}{dx} + \beta_E\frac{d\mu}{dx}\right)A_{NN}^\epsilon D(\epsilon)d\epsilon. \qquad (35)$$

When the system is initially in a hypoequilibrium state, the relationship between the fluctuation A_{NN}^ϵ and the Fermi distribution f is expressed as

$$A_{NN}^\epsilon = \beta_E^{-1}\frac{\partial f}{\partial \epsilon}, \quad \text{with } f = \frac{1}{e^{\beta_E\epsilon + \beta_N} + 1}. \qquad (36)$$

The particle flux can then be rewritten as

$$\begin{aligned}
J_N &= \frac{V\delta x}{A}\int \frac{1}{\tau^\epsilon}\left((\epsilon + \mu)\frac{d\beta_E}{dx} + \beta_E\frac{d\mu}{dx}\right)\beta_E^{-1}\frac{\partial f}{\partial \epsilon}D(\epsilon)d\epsilon \\
&= -\frac{V\delta x}{A}\left(\frac{dE_f^0}{dx} + e\mathcal{E}\right)\int \frac{1}{\tau^\epsilon}\frac{\partial f}{\partial \epsilon}D(\epsilon)d\epsilon \\
&\quad + \frac{V\delta x}{A}\beta_E^{-1}\frac{d\beta_E}{dx}\int \frac{1}{\tau^\epsilon}(\epsilon - E_f)\frac{\partial f}{\partial \epsilon}D(\epsilon)d\epsilon, \qquad (37)
\end{aligned}$$

where $E_f = E_f^0 + e\Phi = -\mu = -\beta_N/\beta_E$, E_f^0 is the fermi level without an external field, $-d\mu = dE_f^0 + ed\Phi$ is the differential chemical potential, and $d\Phi/dx = \mathcal{E}$ is the external field. Here, e and Φ are the electric charge and electric field potential, respectively.

As a comparison, the Boltzmann transport equation (BTE) in the low-field region results in the following particle flux expression [40]:

$$\begin{aligned}
J_N &= -\frac{1}{3}\left(\frac{dE_f^0}{dx} + e\mathcal{E}\right)\int \tau' v^2\frac{\partial f}{\partial \epsilon}D(\epsilon)d\epsilon \\
&\quad - \frac{1}{3T}\frac{dT}{dx}\int \tau' v^2(\epsilon - E_f)\frac{\partial f}{\partial \epsilon}D(\epsilon)d\epsilon, \qquad (38)
\end{aligned}$$

where τ' is the relaxation time in the BTE given by

$$\frac{\partial f}{\partial t} + \frac{\partial \mathbf{r}}{\partial t}\cdot\nabla_{\mathbf{r}}f + \frac{\partial \mathbf{p}}{\partial t}\cdot\nabla_{\mathbf{p}}f = -\frac{f - f_0}{\tau'(\mathbf{r},\mathbf{p})}, \qquad (39)$$

where $\mathbf{r}$ and $\mathbf{p}$ are the particle position and momentum vectors, respectively. f is the particle probability density function and f_0 is its local equilibrium value. The SEAQT and BTE relaxation times τ^ϵ and τ', respectively, are defined by different equations of motion. When the SEAQT relaxation times, the τ^ϵ, are chosen via the relation

$$\frac{V\delta x}{\tau^\epsilon}A = \frac{(\delta x)^2}{\tau^\epsilon} \sim \frac{\tau'(\epsilon)v^2}{3} = \tau'(\epsilon)v_x^2, \qquad (40)$$

i.e.,

$$\tau^\epsilon = \left(\frac{\delta x}{v_x}\right)^2 \Big/ \tau'(\epsilon) = \frac{3m(\delta x)^2}{2\epsilon\tau'(\epsilon)} \qquad (41)$$

the SEAQT equation of motion recovers the BTE in the low-field region and its corresponding particle flux.

B. Phonon transport equation

The SEA transport equation for phonon transfer can be derived in a similar fashion to what was done for electron transport. However, there is no particle number conservation in phonon transport so a different set of conservation laws $\{\tilde{C}(\gamma)\} = \{\tilde{H}, \tilde{I}_1, \ldots, \tilde{I}_m\}$ are used. Assuming as before an initial hypoequilibrium state, the time evolution of energy at location A is expressed as

$$\frac{d\langle E\rangle^A}{dt} = \int \frac{V}{\tau^{A,\epsilon}}\epsilon^2 A_{NN}^{A,\epsilon}\left(\beta_E^{A,\epsilon} - \beta_E\right)D^A(\epsilon)d\epsilon. \qquad (42)$$

In the near-equilibrium realm, it is again assumed that systems A and B are both approximately in stable equilibrium. The three relations for phonons, which are the counterparts to the local equilibrium, energy eigenstructure, and fluctuation assumptions made for electrons [i.e., Eqs. (26), (29), (30) above], are as follows:

$$\beta_E^{A,\epsilon} = \beta_E^A, \quad \beta_E^{B,\epsilon} = \beta_E^B, \qquad (43)$$

$$\tau^{A,\epsilon} = \tau^{B,\epsilon} = \tau^\epsilon, \quad D^A(\epsilon) = D^B(\epsilon) = D(\epsilon), \qquad (44)$$

$$A_{NN}^{A,\epsilon} = A_{NN}^{B,\epsilon} = A_{NN}^\epsilon(\beta_N, \beta_E). \qquad (45)$$

The energy flow from B to A is then given by subtracting from Eq. (42) the corresponding one for system B. Thus,

$$\begin{aligned}
\frac{d\langle E\rangle^A}{dt} - \frac{d\langle E\rangle^B}{dt} &= \frac{V}{A}(\beta_E^A - \beta_E^B)\int \frac{\epsilon^2}{\tau^\epsilon}A_{NN}^\epsilon D(\epsilon)d\epsilon \\
&= \frac{V\delta x}{A}\frac{d\beta_E}{dx}\int \frac{\epsilon^2}{\tau^\epsilon}A_{NN}^\epsilon D(\epsilon)d\epsilon, \qquad (46)
\end{aligned}$$

where the fluctuation A_{NN}^ϵ can be written in terms of the boson distribution, i.e.,

$$A_{NN}^\epsilon = -\frac{k_B T^2}{\epsilon}\frac{\partial f}{\partial T}, \quad \text{with } f = \frac{1}{e^{\beta_E\epsilon} - 1}. \qquad (47)$$

Again, assuming contributions from two interfaces, the energy flux can be written as

$$\begin{aligned}
J_E &= \frac{V\delta x}{A}\frac{d\beta_E}{dx}\int \frac{\epsilon^2}{\tau^\epsilon}\left(-\frac{k_B T^2}{\epsilon}\frac{\partial f}{\partial T}\right)D(\epsilon)d\epsilon \\
&= \frac{V\delta x}{A}\frac{dT}{dx}\int \frac{\epsilon}{\tau^\epsilon}\frac{\partial f}{\partial T}D(\epsilon)d\epsilon \\
&= \frac{dT}{dx}\int \frac{(\delta x)^2}{\tau^\epsilon}\hbar\omega\frac{\partial f}{\partial T}D(\omega)d\omega. \qquad (48)
\end{aligned}$$

Here the integral argument has been converted from the energy ϵ into the frequency ω after the last equal sign. By choosing the relaxation times as before via

$$\tau^\epsilon = \left(\frac{\delta x}{v_x}\right)^2 \Big/ \tau'(\epsilon) \qquad (49)$$

and defining the specific heat per unit frequency as

$$C_\omega = \hbar\omega D(\omega)df/dT \qquad (50)$$

one arrives at the same expression for the thermal conductivity k as that given by the BTE [40], i.e.,

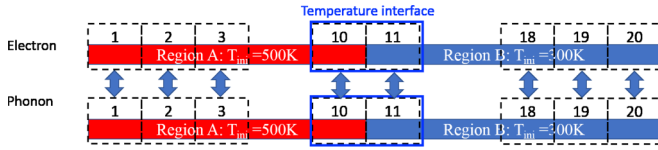$$k = \frac{1}{3}\int \tau' v^2 C_\omega d\omega. \qquad (51)$$

FIG. 1. System definition.

C. Electron-phonon coupling

By assuming a constant relaxation time for phonons τ^p and one for electrons τ^e, the SEAQT framework can recover the two-temperature model (TTM) of electron-phonon coupling [48]. If phonons and electrons have temperatures β_E^p and β_E^e initially, Eqs. (A14) and (A15) reduce to

$$\frac{1}{\tau^p}A_{ES}^p + \frac{1}{\tau^e}A_{ES}^e = \beta_E\left(\frac{1}{\tau^p}A_{EE}^p + \frac{1}{\tau^e}A_{EE}^e\right) + \beta_N\frac{1}{\tau^e}A_{EN}^e, \tag{52}$$

$$\frac{1}{\tau^e}A_{NS}^e = \beta_E\frac{1}{\tau^e}A_{EN}^e + \beta_N\frac{1}{\tau^e}A_{NN}^e, \tag{53}$$

where $A_{XY}^{e(p)}$ is the total fluctuation in a local electron (phonon) system. The Lagrange multiplier $\beta_E = \beta_{E,ep}$ is solved for a system with only electron-phonon coupling such that

$$\beta_E = \frac{\beta_E^e\left(\frac{A_{NN}^e}{\tau^e}\frac{A_{EE}^e}{\tau^e} - \frac{A_{EN}^e}{\tau^e}\frac{A_{EN}^e}{\tau^e}\right) + \beta_E^p\frac{A_{NN}^e}{\tau^e}\frac{A_{EE}^e}{\tau^p}}{\frac{A_{NN}^e}{\tau^e}\frac{A_{EE}^e}{\tau^e} - \frac{A_{EN}^e}{\tau^e}\frac{A_{EN}^e}{\tau^e} + \frac{A_{NN}^e}{\tau^e}\frac{A_{EE}^e}{\tau^p}}$$

$$= \chi\beta_E^e + (1-\chi)\beta_E^p, \tag{54}$$

where clearly β_E is simply a linear combination of β_E^e and β_E^p, and the relation between temperature and fluctuation at equilibrium has been used [30], namely,

$$\beta_E^p = \frac{A_{ES}^p}{A_{EE}^p}, \quad \beta_E^e = \frac{A_{NN}^e A_{ES}^e - A_{EN}^e A_{NS}^e}{A_{NN}^e A_{EE}^e - A_{EN}^e A_{EN}^e}. \tag{55}$$

Here, χ is the coefficient multiplying β_E^e. Excluding a system on the boundary, an electron (phonon) local system in Fig. 1 has interactions with three local systems, i.e., its local upstream system, local downstream system, and local phonon (electron) system. Li and von Spakovsky [30] show that the temperature evolution of a system interacting with multiple systems yields to the SEAQT equation of motion of extensive properties with adjusted parameters, i.e.,

$$\frac{d\beta_E^{e(p)}}{dt} = -\frac{1}{\tilde{\tau}^{e(p)}}\left(\beta_E^{e(p)} - \tilde{\beta}_E^{e(p)}\right), \tag{56}$$

where every interaction with a neighboring system contributes to one term in the calculation of $\tilde{\tau}^{e(p)}$ and $\tilde{\beta}_E^{e(p)}$ such that [30]

$$\frac{1}{\tilde{\tau}^{e(p)}} = \frac{1}{\tau^{e(p)}} + \frac{1}{\tau^{e(p)}} + \frac{1}{\tau^{e(p)}}, \tag{57}$$

$$\frac{\tilde{\beta}_E^e}{\tilde{\tau}^e} = \frac{\beta_{E,ee}^{up}}{\tau^e} + \frac{\beta_{E,ee}^{down}}{\tau^e} + \frac{\beta_{E,ep}}{\tau^e}, \tag{58}$$

$$\frac{\tilde{\beta}_E^p}{\tilde{\tau}^p} = \frac{\beta_{E,pp}^{up}}{\tau^p} + \frac{\beta_{E,pp}^{down}}{\tau^p} + \frac{\beta_{E,ep}}{\tau^p}. \tag{59}$$

Here *Matthiessen's rule* has been used. The subscripts *ee*, *pp*, and *ep* stand for electron diffusion, phonon diffusion, and

electron-phonon coupling, while the *up* and *down* superscripts stand for the interaction with the upstream and downstream local system, respectively. Equation (56) for each electron then takes the form

$$\frac{d\beta_E^e}{dt} = -\frac{3}{\tau^e}\left(\beta_E^e - \frac{1}{3}\left(\beta_{E,ee}^{up} + \beta_{E,ee}^{down} + \beta_{E,ep}\right)\right)$$

$$= -\frac{1}{\tau^e}\left(2\beta_E^e - \beta_{E,ee}^{up} - \beta_{E,ee}^{down}\right) - \frac{1}{\tau^e}\left(\beta_E^e - \beta_{E,ep}\right)$$

$$= \frac{(\delta x)^2}{\tau^e}\frac{d^2\beta_E^e}{dx^2} - \frac{1}{\tau^e}\left[\beta_E^e - \chi\beta_E^e - (1-\chi)\beta_E^p\right],$$

$$\frac{d\beta_E^e}{dt} = \frac{(\delta x)^2}{\tau^e}\frac{d^2\beta_E^e}{dx^2} - \frac{(1-\chi)}{\tau^e}\left(\beta_E^e - \beta_E^p\right), \tag{60}$$

where we have used Eq. (54) in the third equal sign and the fact that the first term to the right of the second equal sign is the finite difference expression for the second order derivative of β_E^e with respect to x. Similarly, the temperature evolution of a phonon is given by

$$\frac{d\beta_E^p}{dt} = \frac{(\delta x)^2}{\tau^p}\frac{d^2\beta_E^p}{dx^2} - \frac{\chi}{\tau^p}\left(\beta_E^p - \beta_E^e\right). \tag{61}$$

Equations (60) and (61) are equivalent to the two temperature model of electron-phonon coupling [48], where the first term to the right of the equal sign in both equations is the heat diffusion and the second term is the phonon-electron coupling.

V. HEAT AND MASS DIFFUSION AT A TEMPERATURE DISCONTINUITY ACROSS A HOMOGENEOUS INTERFACE

The SEAQT transport equations derived in the previous sections are applicable throughout the nonequilibrium region even far from equilibrium and as demonstrated above are completely consistent with the linear BTE transport equations, which are limited to the near-equilibrium realm. In this section, a case study is used to illustrate the general applicability of the SEAQT framework to the multiphysics of far-from-equilibrium processes. The heat and mass diffusion at a temperature discontinuity across a homogeneous interface are modeled. The system is divided into two distinct regions with different initial temperatures (i.e., 300 and 500 K). The relaxation of the system results in electron transport, phonon transport, and electron-phonon coupling. To solve this example problem, two main difficulties must be addressed. First, although the local systems initially are all in local equilibrium states, the local equilibrium condition does not hold during the system state evolution due to a different relaxation time associated with each energy eigenvalue. Thus, it is expected that particles occupying different energy eigenstates have different relaxation times and as a consequence different rates of diffusion. The resulting energy dispersion means that particles with different energies are no longer in mutual equilibrium even in the same local system. Traditional thermodynamic methods are dependent on the local equilibrium assumption and, thus, must fail to accurately predict the correct property values in a nonequilibrium local system.

The second difficulty is that the interaction at the temperature discontinuity across a homogeneous interface is not a quasiequilibrium process. The interface modeled is a

simplification. We assume a small region across which a very large temperature gradient exists. Traditional thermodynamic methods are again limited in studying such a region, since these methods require the near-equilibrium assumption. In contrast, the SEAQT framework does not and is, thus, able to predict evolutions of both nonequilibrium systems and nonquasiequilibrium processes consistent with all the thermodynamic requirements.

The SEAQT model used here divides the system into 20 locations (ten for each region) as depicted in Fig. 1. At each location, there are two local systems: one for the electrons and the other for the phonons. All local systems are allowed to be in nonequilibrium states. Each local system is defined by a set of energy eigenlevels as well as the relaxation time for every single eigenlevel. Practically, the electron eigenlevels (or band structure) can be determined from density functional theory calculations, while the phonon eigenlevels (or dispersion relation) can be found from lattice or molecular dynamic calculations. However, since the focus here is on illustrating the nonequilibrium evolution of state of the system, these cumbersome calculations of the eigenstructure are avoided, and some rather simple models, which can be found in any solid-state physics textbook [49], are used. Furthermore, the SEAQT relaxation time τ^ϵ for each energy eigenlevel (electron or phonon) needed for the nonequilibrium evolution of state is determined from the BTE relaxation time τ' [see Eqs. (41) and (49)], which can be derived from the total scattering rate using Fermi's "golden rule." Since it is the total scattering rate that determines the SEAQT relaxation time τ^ϵ as a property of a given eigenlevel ϵ, all scattering mechanisms contributing to the time evolution of the occupation of that single eigenlevel are taken into account when using the SEAQT equation of motion. This equation, thus, naturally predicts the relaxation trajectories of all eigenlevels, accounting for all of the different coupling mechanisms present.

The electron eigenstructure is calculated from the model of an electron gas in an infinite potential well with dimensions 1 cm by 1 cm by 1 cm. The phonon dispersion relation is determined from a one-dimensional atom chain model with two types of atoms: the one providing an optical branch and the other an acoustic branch. The masses of the atoms are 20 and 10 amu, respectively, with a separation distance of 5 Å. The relaxation time of each energy eigenlevel of electrons (or phonons), which is typically a monotonically decreasing (or increasing) function of the eigenenergy covering several orders of magnitude, is chosen based on $(\tau^\epsilon)^e \propto E^{-0.8}$ [or $(\tau^\epsilon)^{ph} \propto E^{1.2}$] and with a range covering three orders of magnitude (from 0.006 to 1.3 time units) [50]. The initial Fermi level of the electron is chosen to be 0.7049 eV above the ground state.

To study the relaxation of one of the local systems of the network shown in Fig. 1, the energy and mass flows with neighboring local systems at every instant of time must be determined after which the total rate of change of the energy and mass in the given local system can be found. For example, the local system Electron-2 has three neighbors: Electron-1, Electron-3, and Phonon-2. To calculate the contribution of the total mass and energy flow from one of the neighbors, e.g., Electron-1 to Electron-2, the SEAQT equation of motion [Eqs. (21) and (22)] are applied to a composite system consisting of Electron-1 and Electron-2 subject to a specific

set of constraints [30,38]. The mass and energy flow is then treated as a result of the relaxation of the nonequilibrium composite system. The electron transport is solved subject to the constraints $\{\tilde{C}(\gamma)\} = \{\tilde{H}, \tilde{N}, \tilde{I}_a, \ldots, \tilde{I}_m\}$ (Sec. III A), while the phonon transport uses the constraints $\{\tilde{C}(\gamma)\} = \{\tilde{H}, \tilde{I}_a, \ldots, \tilde{I}_m\}$ (Sec. III B). The energy transport between electron and phonon at the same location uses the constraints $\{\tilde{C}(\gamma)\} = \{\tilde{H}, \tilde{N}_e, \tilde{I}_a, \ldots, \tilde{I}_m\}$ for which the electron particle number is conserved but the phonon particle number is not. Using this procedure, the energy and mass flows in the local system networks are determined and the relaxation of the whole network predicted.

Phonon transport without the inclusion of the local electron systems is considered first. The transient temperature profiles of the local systems is plotted in Fig. 2(a). As can be seen, the sharp temperature change at the interface flattens out very quickly (see the temperature curves of local systems 10 and 11) at the very beginning of the transient process. Later on, the energy spreads out to the two ends far away from the
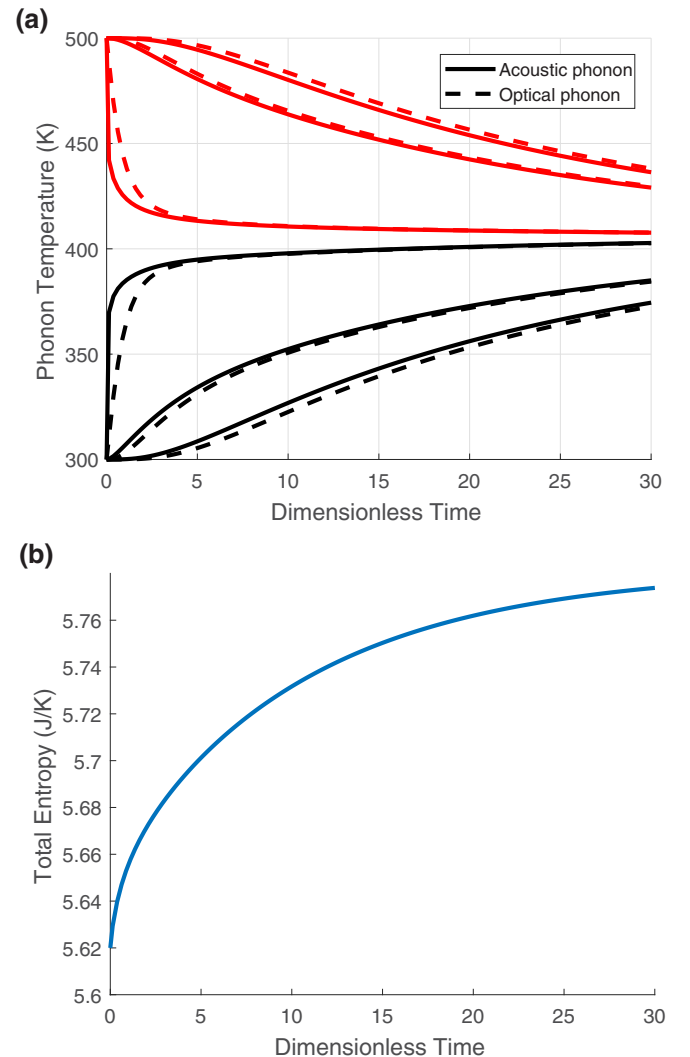

FIG. 2. (a) Transient temperature and (b) entropy evolutions of the system with phonon flow only. Each pair of solid and dashed curves in (a) belongs to a particular local system ordered from top to bottom in the figure by local systems 1, 5, 10, 11, 15, and 20.

interface. The entropy evolution reflects a process in which the largest amount of the entropy generation occurs in the first five units of dimensionless time. It can be understood in the context of the entropy generation σ expressed in terms of the conjugate flux (δQ) and conjugate force [$\Delta(1/T)$] such that $\sigma = (\delta Q)\Delta(1/T)$ and for which the temperature gradient is very big initially. Moreover, as in the figure, the trajectories of the optical and acoustic phonons are different with the acoustic phonon exhibiting the faster energy transport. Because of the temperature difference between the optical and acoustic phonons, the optical phonon is also heated up (or cooled down) by the acoustic phonon during the relaxation. Thus, there is considerable entropy generation inside each local system as well, which cannot be directly described by the relation $\sigma = (\delta Q)\Delta(1/T)$. However, the more general dissipation potential developed in the SEAQT framework provides an explanation using the hypoequilibrium concept. The reader is referred to [28] for details.

When the local electron systems are included, and the system is composed of coupled phonon and electron pathways, the temperature profiles of both the phonons and electrons are those plotted in Fig. 3. The electron temperature plotted uses an average temperature approximately equal to the temperature of the electrons at the Fermi level. Comparing Fig. 3(a) to Fig. 2(a), the optical phonon and acoustic phonon follow almost the same evolutionary trajectories in both figures and are also quite similar to the trajectories of the electrons. However, the coupling with the electrons reduces the difference between optical and acoustic phonon transport as seen in Fig. 3(a). The explanation for this is based on the difference in behavior of fermions and bosons. The Fermi distribution dictates that only the electrons near the Fermi level make a significant contribution to the transport process. Since these electrons are in a rather narrow energy range, all of these electrons have almost the same energy (Fermi energy) and, thus, have a smaller dispersion of energy relative to the electron diffusion speed [40]. As to the bosons, all energy eigenlevels participate in the transport process so that the diffusion speed shows a much larger dispersion of energy. Furthermore, heat interactions with the electrons serve as another resource or sink for the phonons so that the temperature difference among phonon modes is reduced [51].

As a check on the temperature profiles predicted by the SEAQT framework, it can be shown that as expected from conventional Fourier diffusion theory, a linear temperature profile for large times (i.e., at steady state) is recovered under conditions of linearity and a constant heat conduction coefficient. A brief discussion with results is given in Appendix B.

The particle number and energy transport in the system are presented via Fig. 4. Although the local systems are at the same initial Fermi level, the initial temperature difference results in some deviation in the initial particle numbers of the different electron local systems as shown in Fig. 4(a). In the particle number evolution, it is observed that the temperature gradient acts as a diffusion driving force for electron transport, which causes the nonuniform particle number distributions for the whole system at five time units. More details about this phenomenon, including a complete derivation from the SEAQT framework of the Onsager relations for coupled
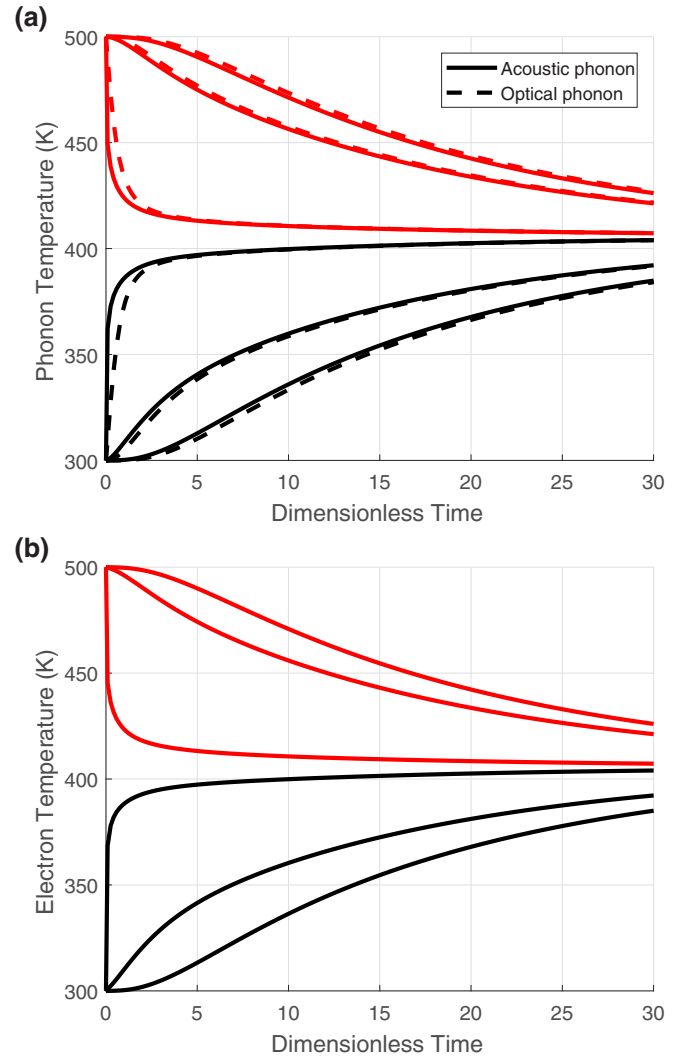

FIG. 3. Transient temperature evolutions of (a) phonons and (b) electrons in an electron-phonon coupling system. Each pair of solid and dashed curves in (a) and each solid curve in (b) belongs to a particular local system ordered from top to bottom in the figure by local systems 1, 5, 10, 11, 15, and 20.

transport, can be found in [28,30]. However, only about 0.1% of all of the electrons move between local systems, which is consistent with the fact that only fermions near the Fermi level participate in the transport.

As to energy transport, Fig. 4(b) shows that the electron energy in one local system only changes less than 1 out of 90 J (the equilibrium energy) from the initial state to the final equilibrium state and that electron energy transport happens relatively fast, i.e., in less than five time units. In contrast, the phonon energy changes by about 25 J out of 60 J (the equilibrium energy) in an evolution that requires more than 30 time units. This comparison supports the fact that phonons, as bosons, account for most of the energy transport, since all phonon modes contribute. Although only a small number of the electrons transport energy, these electrons facilitate the energy transport and heat up (or cool down) the phonons locally. This is
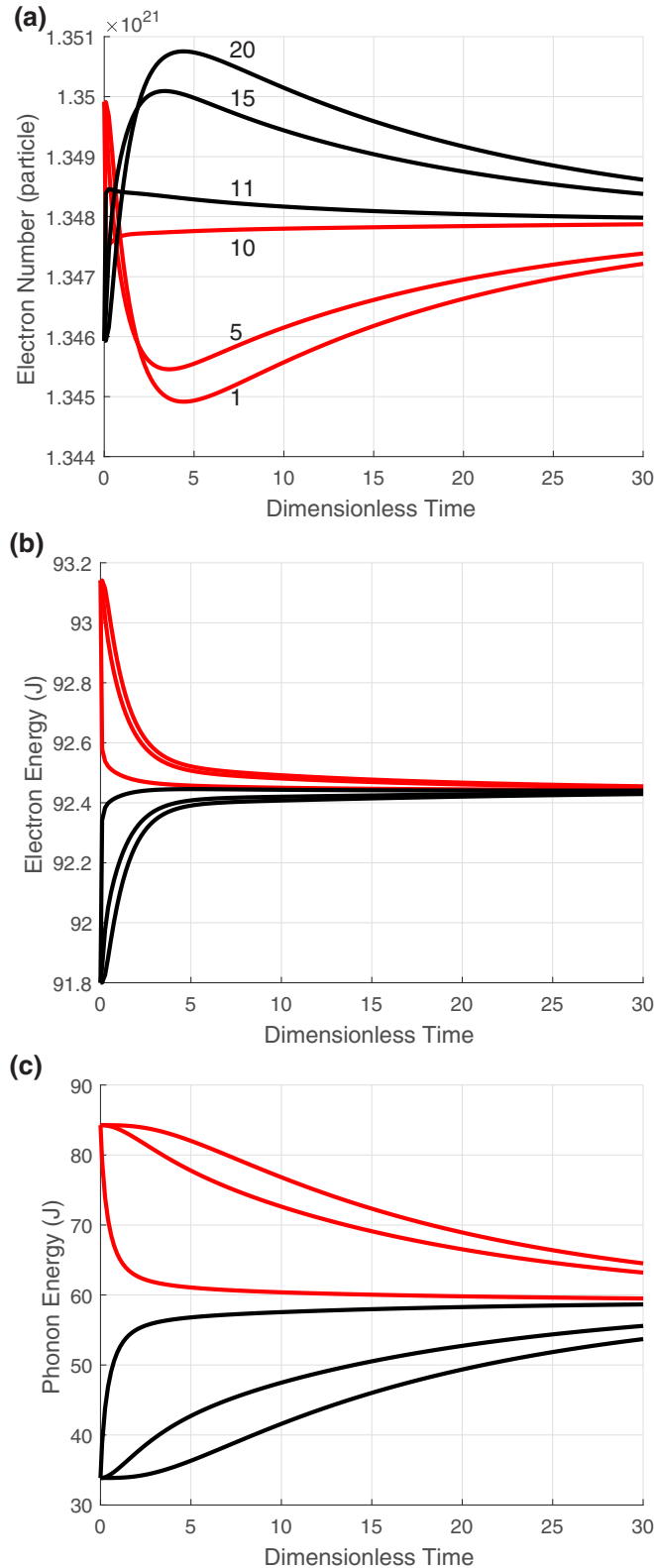
FIG. 4. Transient evolutions of (a) electron number, (b) electron energy, and (c) phonon energy in an electron-phonon coupling system. Each curve belongs to a particular local system ordered from top to bottom in the figures (b) and (c) by local systems 1, 5, 10, 11, 15, and 20.

consistent with the observation above that the electron-phonon coupling can reduce the dispersion in phonon transport.

VI. CONCLUSIONS

This paper presents a framework for studying electron and phonon transport phenomena using SEAQT. This framework is developed based on thermodynamic principles and is thermodynamically rigorous throughout the nonequilibrium realm even that far from equilibrium. The features of the SEAQT framework extend the applicability of thermodynamics to the study of local-nonequilibrium systems as well as nonquasiequilibrium processes. To illustrate this approach, a case study of heat and mass transport at a temperature homogeneous interface where a temperature discontinuity occurs is presented. As demonstrated, the local equilibrium assumption fails when energy dispersion in the transport of different phonon modes is observed. Furthermore, the large entropy generation, which occurs during the transport process at the interface, demonstrates that a quasiequilibrium description of this process would also fail. In contrast, the SEAQT model succeeds in providing a rigorous description and correct prediction of the nonequilibrium thermodynamic evolution. Moreover, the coupling of electron and phonon pathways using the SEAQT model shows that the electrons, which have a much smaller dispersion during the diffusion, reduce the dispersion in phonon transport through electron-phonon interactions.

APPENDIX A: CALCULATION OF MEASUREMENTS

This Appendix explains the process for determining the nonequilibrium measurements of the intensive properties (β_j) from Eq. (13) [30,47]. The functional derivatives of the system properties defined by Eq. (6) take the form

$$|\Psi_k) = 2 \sum_{n^k=1}^{\infty} \gamma_{n^k}^k \hat{e}_{n^k}^k, k = a, \ldots, m, \tag{A1}$$

$$|\Psi_H) = 2 \sum_{k=a}^{m} \sum_{n^k=1}^{\infty} n^k \epsilon^k \gamma_{n^k}^k \hat{e}_{n^k}^k, \tag{A2}$$

$$|\Psi_N) = 2 \sum_{k=a}^{m} \sum_{n^k=1}^{\infty} n^k \gamma_{n^k}^k \hat{e}_{n^k}^k, \tag{A3}$$

$$|\Phi) = 2 \sum_{k=a}^{m} \sum_{n^k=1}^{\infty} \gamma_{n^k}^k \ln p_{n^k}^k \hat{e}_{n^k}^k, \tag{A4}$$

where $\hat{e}_{n^k}^k$ is the unit vector in thermodynamic state space (the space of γ). By defining the probability, energy, particle number, entropy, and fluctuation of the single-particle energy eigenlevels as

$$\langle I \rangle_k = \sum_{n^k=1}^{\infty} p_{n^k}^k = 1, \forall k = a, \ldots, m, \tag{A5}$$

$$\langle N \rangle_k = \sum_{n^k=1}^{\infty} n^k p_{n^k}^k, k = a, \ldots, m, \tag{A6}$$

$$\langle e \rangle_k = \sum_{n^k=1}^{\infty} n^k \epsilon^k p_{n^k}^k, \quad k = a, \dots, m, \tag{A7}$$

$$\langle s \rangle_k = \sum_{n^k=1}^{\infty} p_{n^k}^k \ln p_{n^k}^k, \quad k = a, \dots, m, \tag{A8}$$

$$A_{XY}^k = \langle XY \rangle_k - \langle X \rangle_k \langle Y \rangle_k, \tag{A9}$$

the $m + 2$ conservation laws [Eq. (13)] can be represented as

$$(\Psi_k | \hat{L} | \Phi) = \frac{4}{\tau^k} \langle s \rangle_k = \sum_{j=1}^{m+2} (\Psi_k | \hat{L} | \Psi_j) \beta_j$$
$$= \frac{4}{\tau^k} (\beta_I^k + \beta_E \langle e \rangle_k + \beta_N \langle N \rangle_k), \quad k = 1, \dots, m, \tag{A10}$$

$$(\Psi_H | \hat{L} | \Phi) = \sum_{k=a}^{m} \frac{4}{\tau^k} \langle es \rangle_k = \sum_{j=1}^{m+2} (\Psi_H | \hat{L} | \Psi_j) \beta_j$$
$$= \sum_{k=a}^{m} \frac{4}{\tau^k} (\beta_I^k \langle e \rangle_k + \beta_E \langle ee \rangle_k + \beta_N \langle eN \rangle_k), \tag{A11}$$

$$(\Psi_N | \hat{L} | \Phi) = \sum_{k=a}^{m} \frac{4}{\tau^k} \langle Ns \rangle_k = \sum_{j=1}^{m+2} (\Psi_N | \hat{L} | \Psi_j) \beta_j$$
$$= \sum_{k=a}^{m} \frac{4}{\tau^k} (\beta_I^k \langle N \rangle_k + \beta_E \langle eN \rangle_k + \beta_N \langle NN \rangle_k). \tag{A12}$$

Moreover, for any additive extensive properties C (including e, s, N, A_{XY}), if the system average temperature is relatively high, the summation over k can be replaced by an integral over ϵ such that

$$\sum_k \frac{1}{\tau^k} \langle C \rangle^k = \sum_\epsilon \frac{1}{\tau^\epsilon} \langle C \rangle_\epsilon \frac{\Delta n}{\Delta \epsilon} \Delta \epsilon = V \int d\epsilon \frac{1}{\tau^\epsilon} \langle C \rangle_\epsilon D(\epsilon), \tag{A13}$$

where $D(\epsilon)$ is the density of state per energy per volume.

By subtracting Eq. (A10) from Eqs. (A11) and (A12), one arrives at

$$\sum_{k=a}^{m} \frac{1}{\tau^k} A_{ES}^k = \beta_E \sum_{k=a}^{m} \frac{1}{\tau^k} A_{EE}^k + \beta_N \sum_{k=a}^{m} \frac{1}{\tau^k} A_{EN}^k, \tag{A14}$$

$$\sum_{k=a}^{m} \frac{1}{\tau^k} A_{NS}^k = \beta_E \sum_{k=a}^{m} \frac{1}{\tau^k} A_{EN}^k + \beta_N \sum_{k=a}^{m} \frac{1}{\tau^k} A_{NN}^k, \tag{A15}$$

from which β_E and β_N can be determined. Then, β_I^k can be found by Eq. (A10).
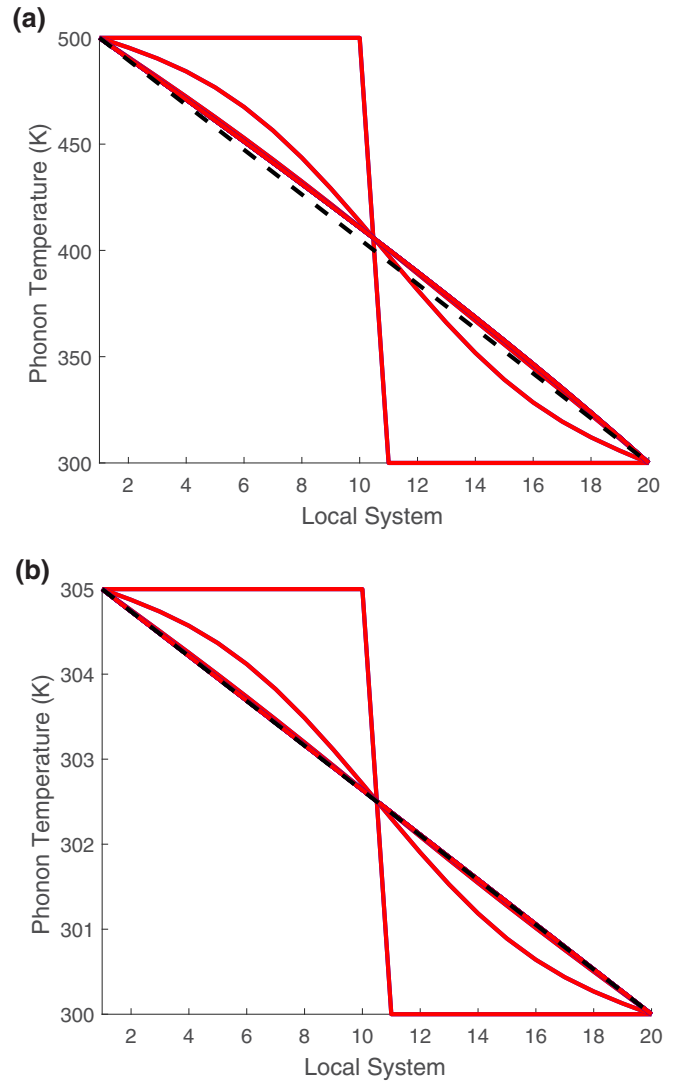

FIG. 5. From the initial transient state to steady state of the phonons. Reservoir temperatures are (a) (300, 500 K) and (b) (300, 305 K). The dashed line is linear.

APPENDIX B: RECOVERING CONVENTIONAL FOURIER DIFFUSION THEORY

Results for the steady states of two systems linked to two different combinations of reservoirs are shown in Fig. 5. If the temperature difference between the two reservoirs is large (such as in the case of Fig. 5(a) with 300 and 500 K for the reservoirs, respectively), the steady-state temperature profile is close to linear, but not quite since the SEAQT framework intrinsically accounts for a temperature-dependent heat conduction coefficient. Higher temperatures result in higher (nonlinear) heat conduction so that the temperature profile is concave as shown in Fig. 5(a). On the other hand, if the reservoir temperatures are close (such as in the case of Fig. 5(b) with 300 and 305 K for the reservoirs, respectively), the temperature profile is linear as seen in Fig. 5(b).

[1] D. C. Rapaport, *The Art of Molecular Dynamics Simulation* (Cambridge University Press, Cambridge, England, 2004).

[2] S. Chen and G. D. Doolen, Annu. Rev. Fluid Mech. **30**, 329 (1998).

[3] P. Vogl and T. Kubis, J. Comput. Electron. **9**, 237 (2010).

[4] A. Rossani and G. Kaniadakis, Physica A **277**, 349 (2000).

[5] A. L. Garcia and W. Wagner, Phys. Rev. E **68**, 056703 (2003).

[6] J. M. Torres-Rincon, in *Hadronic Transport Coefficients from Effective Field Theories* (Springer, New York, 2014), pp. 33–45.

[7] M. E. J. Newman and G. T. Barkema, *Monte Carlo Methods in Statistical Physics* (Oxford University Press, New York, 1999).

[8] U. Seifert, Rep. Prog. Phys. **75**, 126001 (2012).

[9] R. Kubo, M. Toda, and N. Hashitsume, *Statistical Physics II: Nonequilibrium Statistical Mechanics* (Springer Science & Business Media, New York, 2012), Vol. 31.

[10] C. Cercignani, *Theory and Application of the Boltzmann Equation* (Scottish Academic Press, Eidingurgh, 1975).

[11] S. R. de Groot and P. Mazur, *Non-equilibrium Thermodynamics* (North-Holland, Amsterdam, 1962).

[12] S. R. De Groot and P. Mazur, *Non-equilibrium Thermodynamics* (Dover Publications, New York, 2013).

[13] I. Gyarmati, E. Gyarmati, and W. F. Heinz, *Non-equilibrium Thermodynamics* (Springer, New York, 1970).

[14] D. Jou, J. Casas-Vázquez, and G. Lebon, *Extended Irreversible Thermodynamics* (Springer, New York, 1996).

[15] M. Grmela and H. C. Öttinger, Phys. Rev. E **56**, 6620 (1997).

[16] H. C. Öttinger and M. Grmela, Phys. Rev. E **56**, 6633 (1997).

[17] N. Kondo, T. Yamamoto, and K. Watanabe, e-J. Surf. Sci. Nanotechnol. **4**, 239 (2006).

[18] O. Muscato and V. Di Stefano, J. Appl. Phys. **110**, 093706 (2011).

[19] O. Muscato and V. Di Stefano, J. Comput. Electron. **11**, 45 (2012).

[20] G. Chen, Phys. Rev. B **57**, 14958 (1998).

[21] G. P. Beretta, E. P. Gyftopoulos, J. L. Park, and G. N. Hatsopoulos, Nuovo Cimento B (1971–1996) **82**, 169 (1984).

[22] G. P. Beretta, E. P. Gyftopoulos, and J. L. Park, Nuovo Cimento B (1971–1996) **87**, 77 (1985).

[23] G. P. Beretta, Phys. Rev. E **73**, 026113 (2006).

[24] G. P. Beretta, Rep. Math. Phys. **64**, 139 (2009).

[25] G. P. Beretta, Phys. Rev. E **90**, 042113 (2014).

[26] A. Montefusco, F. Consonni, and G. P. Beretta, Phys. Rev. E **91**, 042138 (2015).

[27] G. Li and M. R. von Spakovsky, Phys. Rev. E **93**, 012137 (2016).

[28] G. Li and M. R. von Spakovsky, Phys. Rev. E **94**, 032117 (2016).

[29] G. Li and M. R. von Spakovsky, Energy **115**, 498 (2016).

[30] G. Li and M. R. von Spakovsky, arXiv:1601.02703.

[31] G. Li, O. Al-Abbasi, and M. R. von Spakovsky, J. Phys.: Conf. Ser. **538**, 012013 (2014).

[32] S. Cano-Andrade, G. P. Beretta, and M. R. von Spakovsky, Phys. Rev. A **91**, 013848 (2015).

[33] S. Cano-Andrade, M. R. von Spakovsky, and G. P. Beretta, in *ASME 2013 International Mechanical Engineering Congress and Exposition* (San Diego, CA, USA, 2013), pp. V08BT09A043–V08BT09A043.

[34] G. P. Beretta, O. Al-Abbasi, and M. R. von Spakovsky, Phys. Rev. E **95**, 042139 (2017).

[35] M. von Spakovsky and J. Gemmer, Entropy **16**, 3434 (2014).

[36] C. E. Smith and M. R. von Spakovsky, J. Phys.: Conf. Ser. **380**, 012015 (2012).

[37] G. Li and M. R. von Spakovsky, J. Heat Transfer **139**, 122003 (2017).

[38] G. Li and M. R. von Spakovsky, in *ASME 2015 International Mechanical Engineering Congress and Exposition* (Houston, TX, USA, 2015), p. IMECE2015-53726.

[39] G. Li, M. R. von Spakovsky, C. Shen, and C. Lu, J. Non-Equilib. Thermodyn. **43**, 21 (2017).

[40] G. Chen, *Nanoscale Energy Transport and Conversion* (Oxford University Press, New York, 2005).

[41] Z. Tian, K. Esfarjani, and G. Chen, Phys. Rev. B **86**, 235304 (2012).

[42] X. Li and R. Yang, Phys. Rev. B **86**, 054305 (2012).

[43] E. Tea, J. Huang, and C. Hin, J. Phys. D **49**, 095304 (2016).

[44] J. Huang, E. Tea, G. Li, and C. Hin, Appl. Surf. Sci. **406**, 128 (2017).

[45] E. Tea, J. Huang, G. Li, and C. Hin, J. Chem. Phys. **146**, 124706 (2017).

[46] M. D. Losego, M. E. Grady, N. R. Sottos, D. G. Cahill, and P. V. Braun, Nat. Mater. **11**, 502 (2012).

[47] G. Li, G. P. Beretta, and M. R. von Spakovsky (unpublished).

[48] Y. Wang, X. Ruan, and A. K. Roy, Phys. Rev. B **85**, 205311 (2012).

[49] C. Kittle, *Introduction to Solid State Physics*, 8th ed. (Wiley, New York, 2005).

[50] To facilitate the illustration in our paper, the SEAQT relaxation time τ^ϵ for electrons (or phonons) has been purposely picked to be a monotonically decreasing (or increasing) function of the energy covering three orders of magnitude (from 0.006 to 1.3 time units). A strict selection of the SEAQT relaxation times τ^ϵ should be based on Eqs. (41) and (49) along with information on the BTE relaxation time τ'. For electrons, the selected τ^ϵ corresponds to a relatively weak dispersion in the BTE relaxation time τ', where ϵ in the denominator of Eq. (41) results in a decreasing function of τ^ϵ. In terms of phonons, most materials exhibit a BTE relaxation time τ' that is a decreasing function of the energy $[(\tau')^{\text{optical}} < (\tau')^{\text{acoustic}}]$ and a group velocity of the optical phonons that is smaller than that of the acoustic phonons $(v_x^{\text{optical}} < v_x^{\text{acoustic}})$. Thus, according to Eq. (49), $(\tau^\epsilon)^{\text{acoustic}} < (\tau^\epsilon)^{\text{optical}}$ for the SEAQT phonon relaxation times.

[51] Since the relaxation times for the phonons and electrons are both functions of the energy and since all phonon modes participate in the energy transfer, there is quite a large temperature deviation among the different phonon modes due to their different relaxation times. In contrast, only electrons near the Fermi level participate in the energy transfer and have almost the same relaxation time so that these electrons have almost the same temperature in one local system. If an electron pathway is added to a phonon-only system (Fig. 1 of the paper), electrons with the same temperature will interact with phonons locally. In this case, a phonon-electron-phonon interaction and a phonon-phonon interaction exist at the same time and result in a faster energy transfer locally between phonons than would be the case if only a phonon-phonon interaction were present.